a bridge. Other comparisons between the frequencies of $\tilde{a}^3B_1$ and $\tilde{X}^1A_1$ bicyclobutene are instructive too, but the key feature of the vibrational frequencies in Table VII is that there are no imaginary frequencies for ring-breaking modes. Thus, $^3B_1$ bicyclobutene is predicted to be a relative minimum on the C_4H_4 potential energy surface with either D_{2h} or C_{2v} symmetry.

The adiabatic excitation energy for the transition $(C_{2v})\ \tilde{X}^1A_1 \rightarrow (C_{2v})\ \tilde{a}^3B_1$ is 45.8 kcal/mol at the SCF level and 49.2 kcal/mol at the CISD level. The corresponding $(D_{2h})\ \tilde{X}^1A_1 \rightarrow (D_{2h})\ \tilde{a}^3B_1$ results are 32.9 and 35.8 kcal/mol, respectively. The 13-kcal/mol reduction in the latter two values is primarily due to the energy difference between the C_{2v} and D_{2h} conformations of the ground state; thus, regardless of whether the $\tilde{a}^3B_1$ state actually has a D_{2h} minimum, the $(C_{2v})\ \tilde{X}^1A_1 \rightarrow \tilde{a}^3B_1$ adiabatic excitation energy should be near 17500 cm^{-1}, or 50 kcal/mol. Utilizing DZ SCF geometries,[42] the 6-31G* CISD $(D_{2h})\ N(\pi^2) \rightarrow (D_{2h})\ T(\pi\pi^*)$ adiabatic excitation energy for ethylene is 78.8 kcal/mol. (The corresponding $(D_{2h})\ N(\pi^2) \rightarrow (D_{2d})\ T(\pi\pi^*)\ C_2H_4$ value of 62.0 kcal/mol is less pertinent since $^3B_1$ bicyclobutene is not twisted.) Thus, while the singlet–triplet splitting in bicyclobutene is indeed smaller than that in ethylene, the data in Table VII show that the $\tilde{a}^3B_1$ state of bicyclobutene lies over 30 kcal/mol above the ground state even at the $\tilde{X}^1A_1$ transition state to inversion. The $\tilde{a}^3B_1$ state should not be a factor in the chemistry of bicyclobutene unless it is photochemically populated.

Finally, we find the $\pi^2\sigma\sigma^*$ triplet state to be 80.8 kcal/mol (6-31G* SCF) above the $\sigma^2\pi\pi^*$ ($^3B_1$) triplet state at the $^3B_1$ D_{2h} optimum geometry. However, the $\sigma\pi\pi^*\sigma^*$ quintet state is much lower in energy. At the 6-31G* SCF level, this quintet state ($^5B_{2g}$) has a D_{2h} optimum geometry of R = 1.521 Å, S = 2.030 Å, T = U = 1.087 Å, and $\alpha = \beta$ = 125.7° (as defined in Table VII). An analytic SCF second derivative calculation shows this D_{2h} stationary point to be a relative minimum. The lowest frequency (301 cm^{-1}) corresponds to ring puckering, and a frequency of 887 cm^{-1} is found for stretching the C–C distance S, a mode which should be considered a ring-bending mode. The $^5B_{2g}$ state can aptly be described as two triplet methylene units high-spin coupled across a four-carbon ring. The $^5B_{2g}$ optimum SCF energy (−153.54177) is only 3.6 kcal/mol above the optimum (C_{2v}) $^3B_1$ energy, but, as one would expect, the inclusion of electron correlation increases this energy difference to 27.2 kcal/mol [E(CISD) = −153.94805], giving a CISD adiabatic excitation energy of 76.4 kcal/mol for the $\tilde{X}^1A_1 \rightarrow {}^5B_{2g}$ transition.

Acknowledgment. The research performed at Berkeley was supported by the U. S. National Science Foundation, Grant No. CHE-8218785. This material is also based upon work supported under a National Science Foundation Graduate Fellowship held from 1983 to 1986 by W.D.A. The computations done at Vanderbilt were supported in part by the U. S. National Science Foundation, Grant No. CHE-8605951. We are also grateful to a referee for suggesting the calculations on the triplet state of bicyclobutene.

Registry No. 1, 1120-53-2; **2**, 157-39-1; **3**, 1120-53-2; **5**, 58208-49-4; vinylacetylene, 689-97-4.

(42) Yamaguchi, Y.; Osamura, Y.; Schaefer, H. F. *J. Am. Chem. Soc.* **1983**, *105*, 7506.

(43) Cotton, F. A. *Chemical Applications of Group Theory*, 2nd ed.; Wiley-Interscience: New York, 1971; pp 354–364.

Non-Kekulé Acenes. The Dimethylenepolycyclobutadienes, a New Class of (4*n* + 2) Alternant Hydrocarbons

Julianto Pranata and Dennis A. Dougherty*[1]

Contribution No. 7443 from the Arnold and Mabel Beckman Laboratory of Chemical Synthesis, California Institute of Technology, Pasadena, California 91125. *Received July 17, 1986*

Abstract: The dimethylenepolycyclobutadienes (3_n) are the non-Kekulē analogues of the classical acenes. Application of a variety of theoretical methods reveals several novel features of such structures. Most interesting is the emergence of a parity rule. When n is even, 3_n is predicted to be a singlet, with n disjoint NBMO's. When n is odd, theory predicts a triplet ground state with (n + 1) NBMO's that are not fully disjoint.

Interest in new organic materials with unusual optical, magnetic, and electronic properties continues to grow. Polyacetylene (**1**) provides a powerful paradigm for the development of such structures. One starts with a simple monomer with a relatively large HOMO–LUMO energy gap, and builds up highly extended, conjugated π systems. As the chain grows, the HOMO–LUMO energy gap decreases, and when this gap becomes small enough, novel properties must emerge. This approach has led to the development of many new materials such as poly(p-phenylene), poly(p-phenylene sulfide), polythiophene, etc. Another related example is provided by the classical acenes (**2**) (benzene, naphthalene, anthracene, ...). The smaller acenes are, of course, well-known and extensively studied. Recent theoretical and experimental work on larger acenes with $n > 7$ suggests that such structures could have very intriguing properties.[2]

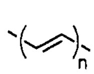

1

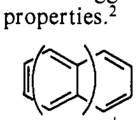

2

An alternative strategy for building novel structures would be to start with a monomer that has essentially no HOMO–LUMO gap. With this approach, one would expect that the onset of unusual properties would occur for a "polymer" of much shorter chain length. Non-Kekulē molecules provide attractive candidates for such a monomer. A wide variety of non-Kekulē structures has been prepared in recent years,[3] including some that are remarkably stable.[3b] Such structures can be either paramagnetic

(1) Fellow of the Alfred P. Sloan Foundation, 1983–1985; Camille and Henry Dreyfus Teacher-Scholar, 1984–1989.

(2) Kivelson, S.; Chapman, O. L. *Phys. Rev. B* **1983**, *28*, 7236–7243. Chapman, O. L.; Seminar, California Institute of Technology, March 19, 1986.

(3) (a) Trimethylenemethane: Dowd, P. *Acc. Chem. Res.* **1972**, *5*, 242–248. Dowd, P.; Chow, M. *Tetrahedron*, **1982**, *38*, 799–807. (b) 2-Alkylidene-1,3-cyclopentanediyls: Berson, J. A. *Acc. Chem. Res.* **1978**, *11*, 446–453. Berson, J. A. In *Diradicals*; Borden, W. T., Ed.; Wiley: New York, 1982; pp 151–194. (c) Tris-*N*-methyliminomethane: Quast, H.; Bieber, L.; Danen, W. C. *J. Am. Chem. Soc.* **1978**, *100*, 1306–1307. (d) *m*-Xylylene and *m*-quinomethane: Platz, M. S. In *Diradicals*, ref 3b, pp 195–222. Rule, M.; Matlin, A. R.; Seeger, D. E.; Hilinski, E. F.; Dougherty, D. A.; Berson, J. A. *Tetrahedron* **1982**, *38*, 787–798. (e) 1,8-Naphthoquinomethane and related structures: Platz, M. S. In *Diradicals*, ref 3b, pp 222–255. Platz, M. S.; Carrol, G.; Pierrat, F.; Zayas, J.; Auster, S. *Tetrahedron* **1982**, *38*, 777–785. (f) Tetramethyleneethanes: Dowd, P. *J. Am. Chem. Soc.* **1970**, *92*, 1066–1068. Roth, W. R.; Erker, G. *Angew. Chem., Int. Ed. Engl.* **1973**, *12*, 503–504.

0002-7863/87/1509-1621$01.50/0

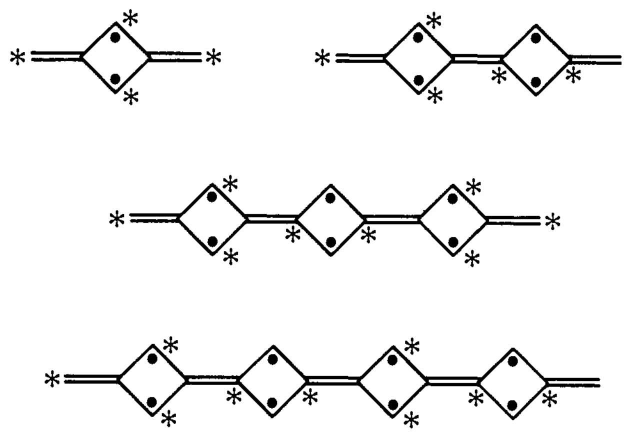

Figure 1. The non-Kekulé acenes as alternant hydrocarbons.

or diamagnetic, and many display novel spectral properties.

Our own interest in such molecules arose from our recent synthesis[4] and spectroscopic characterization[5] of the non-Kekulé isomer of benzene, 2,4-dimethylene-1,3-cyclobutanediyl (**3**$_1$). This structure has a triplet ground state and is orange, with λ_{max} 506 nm, ϵ_{max} 8000 M^{-1} cm^{-1}.[5] Thus, remarkable changes in electronic structure occur on converting benzene (λ_{max} 254 nm) to its non-Kekulé isomer.

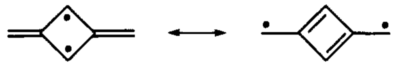

3$_1$

If **3**$_1$ is non-Kekulé benzene, what is non-Kekulé naphthalene? The answer is **3**$_2$, a $C_{10}H_8$, 10 π electron system. One can envision a series of $(4n + 2)$ π systems as shown in **3**$_n$. These are the non-Kekulé acenes. In the present work we describe the remarkable electronic structures of the smaller members of this series. There are substantial qualitative differences between the non-Kekulé acenes **3**$_n$ and the classical acenes **2**, and it is apparent that very unusual properties could arise from structures such as **3**$_n$ even for relatively small values of n. We also describe some very preliminary results for the infinite non-Kekulé acene, a quite novel polymer.

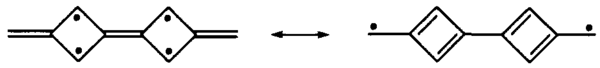

3$_2$

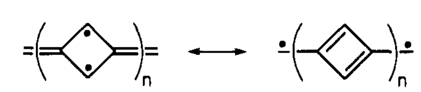

3$_n$

Qualitative Analysis

Structure-Based Methods. Like their classical analogues, the non-Kekulé acenes are alternant hydrocarbons (AH). That is, their atoms can be divided into two sets, termed starred and unstarred, such that no two atoms of the same set are connected. However, Figure 1 illustrates an important difference between classical and non-Kekulé acenes. For all the classical acenes (**2**) the number of starred atoms equals the number of unstarred. The non-Kekulé "monomer" **3**$_1$, however, has four starred and two unstarred atoms (Figure 1). It has been proposed that such structures will have triplet (T) ground states,[6] a prediction that is supported by our experimental efforts.[4] Borden and Davidson have provided an elegant rationalization of this effect.[7] Monomer **3**$_1$ has two nonbonding molecular orbitals (NBMO). It can be shown[8] that when an AH has unequal numbers of starred and unstarred atoms, the NBMO's are confined to the larger set. In most cases, including **3**$_1$, this means that the NBMO's are *not* disjoint; i.e., they span common atoms. This leads to unfavorable exchange repulsions in the singlet (S) producing a triplet ground state. We shall refer to this type of analysis as the disjoint NBMO approach.

Table I. NBMO's of Non-Kekulé Acenes (**3**n) Obtained from HMO Calculations

n	no. of NBMO's	n	no. of NBMO's
1	2	4	4
2	2	5	6
3	4	6	6

While naphthalene represents a relatively straightforward extension of benzene, the $n = 2$ non-Kekulé acene (**3**$_2$) is *qualitatively* different from the $n = 1$ structure. Now the number of starred atoms equals the number of unstarred (Figure 1). In such a case the NBMO's *are* disjoint, with one NBMO confined to the starred, and the other confined to the unstarred atoms. To first order S and T are degenerate. Typically, higher order effects preferentially stabilize S, making it the ground state. It is easy to see from Figure 1 that a parity rule exists for the non-Kekulé acenes. When n is odd, there are two more starred atoms than unstarred, and a triplet ground state is predicted by the disjoint NBMO approach. When n is even, there are equal numbers of starred and unstarred atoms, and a singlet ground state is expected.

Note that all these structures (**3**$_n$) are non-Kekulé, in that the resonance structure with maximal pairing of electrons into bonds still has two unpaired electrons.[9] It has been proposed that an alternative approach to predicting ground spin states of alternant hydrocarbons is to simply count the unpaired spins in this resonance structure. This is termed classical structure theory.[6b] Thus, these two qualitative approaches produce conflicting predictions. Classical structure theory predicts T < S for all non-Kekulé acenes, while the disjoint NBMO analysis predicts T < S for odd n and S < T for even n. In the following section, we will see that Hückel theory, as conventionally applied, leads to still another prediction.

Hückel Molecular Orbital Theory (HMO). The HMO results for **3**$_1$ are well-known and produce an MO pattern with two degenerate NBMO's. We have applied HMO to the other non-Kekulé acenes, and for the present we shall focus on the NBMO's. The relevant data are summarized in Table I. It is immediately apparent that HMO has uncovered a second manifestation of the parity rule. When n is even, there are n strictly degenerate ($E = \alpha$) NBMO's; when n is odd, there are $(n + 1)$ NBMO's. Thus, structure **3**$_n$ (even n) contains n, degenerate, half-filled, nonbonding MO's. Yet, the disjoint NBMO method predicts a singlet ground state! The properties of such a substance must be quite remarkable.

HMO alone does not lead to predictions of ground spin states. The most common approach for predicting spin states of organic molecules has been to couple HMO with Hund's first rule. The relative merits of this approach have been the topic of much recent discussion,[10] and we simply note here that the HMO/Hund analysis leads to predictions for the non-Kekulé acenes very different from the structure-based methods. All structures are predicted to be high spin, and, with large n, *very* high spin structures are expected. For example, **3**$_3$ and **3**$_4$ should be quintets, **3**$_5$ and **3**$_6$ septets, etc.

The nature of the NBMO's predicted by HMO is also quite interesting. We defer our discussion of these to the next section, in which more quantitative results are described.

(4) Snyder, G. J.; Dougherty, D. A. *J. Am. Chem. Soc.* **1985**, *107*, 1774–1775. More recently, **3**$_1$ has been generated from a second precursor: Dowd, P.; Paik, Y. H. *Ibid.* **1986**, *108*, 2788–2790.

(5) Snyder, G. J.; Dougherty, D. A. *J. Am. Chem. Soc.* **1986**, *108*, 299–300.

(6) For recent discussions of such rules, see: (a) Ovchinnikov, A. A. *Theor. chim. Acta* **1978**, *47*, 297–304. (b) Klein, D. J.; Nelin, C. J.; Alexander, S.; Matsen, F. A. *J. Chem. Phys.* **1982**, *77*, 3101–3108.

(7) Borden, W. T.; Davidson, E. R. *J. Am. Chem. Soc.* **1977**, *99*, 4587–4594.

(8) Borden, W. T. In *Diradicals*, ref 3b, pp 1–72.

(9) Dewar, M. J. S. *The Molecular Orbital Theory of Organic Chemistry*; McGraw-Hill: New York, 1969; pp 232–233.

(10) Seeger, D. E.; Lahti, P. M.; Rossi, A. R.; Berson, J. A. *J. Am. Chem. Soc.* **1986**, *108*, 1251–1265.

Table II. S–T Gaps[a] (kcal/mol) in Non-Kekulē Acenes[b]

	NCI	NSCI	NSDCI	2-level SCI	3-level SCI	4-level SCI
3$_1$	19.5	8.2	5.1	20.7		
3$_2$	−0.03	−0.02	−0.06	−2.0	−4.0	−1.5
3$_3$	8.8	1.8	1.9			
3$_4$	−0.02	−0.13				

[a] A positive value indicates T < S. [b] See Appendix for a description of the various levels of theory.

Table III. Calculated Electronic Transitions[a] for **3**$_1$

	NSCI	NSDCI	SCI
	Triplet Transitions		
$B_{2u} \rightarrow B_{1g}$ (allowed)[b]	501 (0.018)	501 (0.018)	504 (0.008)
$B_{2u} \rightarrow B_{3u}$ (forbidden)	333	336	363
$B_{2u} \rightarrow B_{2u}$ (forbidden)	225	225	302
$B_{2u} \rightarrow B_{3u}$ (forbidden)	306	309	283
$B_{2u} \rightarrow A_g$ (allowed)			277 (0.009)
	Singlet Transitions		
$A_g \rightarrow B_{2u}$ (allowed)	1582 (0.003)	1351 (0.003)	32649 (0.0)
$A_g \rightarrow B_{1g}$ (forbidden)	586	551	910
$A_g \rightarrow A_g$ (forbidden)	506	589	514
$A_g \rightarrow B_{1g}$ (forbidden)	243	237	255
$A_g \rightarrow B_{3u}$ (allowed)	204 (0.945)	215 (0.790)	218 (1.331)

[a] In nm; values in parentheses are oscillator strengths. [b] Experimental 506 (0.025) (ref 5).

Quantitative Results. PPP Calculations on 3$_1$

The qualitative schemes described above produce some fascinating, and conflicting predictions for the non-Kekulē acenes. We have applied PPP theory to test and expand upon the qualitative results.[11] This π-only procedure is an SCF method, and thus includes the two-electron terms neglected by HMO. We have also included substantial configuration interaction (CI), as is always necessary for reliable studies of non-Kekulē molecules.[12] We emphasize from the start that we do not expect PPP theory to make quantitatively accurate predictions of the properties of non-Kekulē acenes. It should, however, predict the basic trends along the series properly and provide a basis for evaluating the predictions of the highly qualitative theories described above. The details of the computational procedures and several benchmark calculations are described in the Appendix.

The "monomer" (**3**$_1$) is a crucial structure for this study, since valuable experimental data are available for comparison with computational results. Several ab initio results for **3**$_1$ also provide useful calibration data.[13] Table II presents the calculated S–T gaps (a positive number indicates T < S), and Table III the transition energies and oscillator strengths for **3**$_1$. At any level, **3**$_1$ is calculated to have a substantial triplet preference, as predicted by all the qualitative models and supported by experiment. Several ab initio estimates of the magnitude of the S–T gap in **3**$_1$ have appeared.[13] The values vary somewhat, depending primarily on the geometries used. We have used the π-CI geometry of Davidson et al. Also, our method calculates the vertical S–T gap (i.e., S and T at the same geometry).[13a] The best ab initio estimate of this number is ca. 24 kcal/mol. When S and T are optimized separately (but planarity maintained), a value as low as 8 kcal/mol can be obtained. We conclude that PPP has performed quite well in predicting the S–T gap of **3**$_1$.

The prediction of the optical transition in **3**$_1$ is remarkably good (Table III). Both the energy and the oscillator strength are calculated as accurately as one could possibly hope, given the level of theory involved. The transition is $^3B_{2u} \rightarrow {}^3B_{1g}$, and the dominant configurations involved are shown in Figure 2. It is a symmetry allowed, $\pi \rightarrow \pi^*$ transition. Its relatively weak oscillator strength arises from the fact that it is a so-called "parity forbidden" transition.[14] An interesting additional result of these studies is the prediction of no allowed absorption in the UV/vis region for the singlet state of **3**$_1$.

(11) Pariser, R.; Parr, R. G. *J. Chem. Phys.* **1953**, *21*, 466–471, 767–776. Pople, J. A. *Trans. Faraday Soc.* **1953**, *49*, 1375–1385.
(12) Gisin, M.; Wirz, J. *Helv. Chim. Acta* **1983**, *66*, 1556–1568.
(13) (a) Davidson, E. R.; Borden, W. T.; Smith, J. *J. Am. Chem. Soc.* **1978**, *100*, 3299–3302. (b) Feller, D.; Davidson, E. R.; Borden, W. T. *Ibid.* **1982**, *104*, 1216–1218. (c) Borden, W. T.; Davidson, E. R.; Feller, D. *Tetrahedron* **1982**, *38*, 737–739.

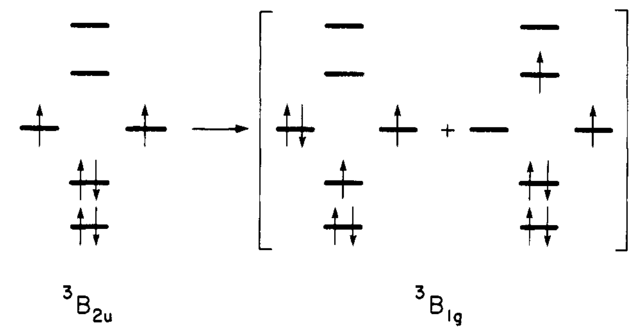

Figure 2. Dominant configurations involved in the first electronic transition of **3**$_1$. The molecule is in the *xy* plane, with the *x*-axis along the long molecular axis.

The important conclusion from the studies on **3**$_1$ is that PPP theory, as presently applied, is in excellent agreement with all available data on **3**$_1$. We thus feel it should provide meaningful predictions of at least the trends and qualitative features of the non-Kekulē acene series.

PPP Results for Higher Non-Kekulē Acenes (3$_2$–3$_6$)

A. NBMO's. One of the most fascinating predictions of HMO is the NBMO pattern of the non-Kekulē acenes (Table I). The prediction is completely confirmed by PPP theory. The orbital energy patterns for **3**$_1$–**3**$_6$ are shown in Figure 3 and the NBMO's are depicted in Figure 4. These SCF calculations were done for the high spin states suggested by Table I, i.e., triplet for **3**$_1$ and **3**$_2$, quintet for **3**$_3$ and **3**$_4$, etc. It could be argued that by imposing high spin states we forced the NBMO patterns shown. However, SCF calculations on lower spin states produced unreasonable results, such as orbitals that did not have appropriate symmetries. Calculations on **3**$_1$ and **3**$_2$ with quintet spin states produced orbital patterns that were basically like those of Figure 3.

Examination of the NBMO's (the PPP and HMO orbitals are essentially identical) reveals another manifestation of the parity rule. When *n* is even all *n* NBMO's are confined exclusively to the CH carbons and all are antisymmetric (A) with respect to the symmetry plane that is perpendicular to the molecular plane and contains the long axis (Figure 4). These orbitals would appear to suggest the resonance structure on the left of structure **3**$_n$ (however, see below). When *n* is odd, there are *n* orbitals of the type just described (A) plus one more that is symmetric (S) with respect to the previously mentioned symmetry plane (Figure 4).[15]

B. S–T Gaps. The different qualitative theories make different predictions concerning ground spin states. Both classical structure theory and HMO/Hund predict T < S for **3**$_2$, while the disjoint NBMO approach predicts S < T. We have thus made a considerable effort to evaluate the spin preference of **3**$_2$. *All* levels of PPP–CI theory predict S < T, consistent only with the disjoint NBMO approach. The results are summarized in Table II. The gap is quite small at the lower levels of theory, but increases substantially as more CI is included.

We have also performed CI calculations at several levels on **3**$_3$ and **3**$_4$ (Table II). Again a parity rule is evident. When *n* is even, we obtain S < T; when *n* is odd, we obtain T < S. Only disjoint NBMO theory predicts this trend, and we consider this an impressive verification of the Borden–Davidson analysis.[7]

C. Electronic Transitions for 3$_2$. An important result of these studies is that **3**$_2$ should have a singlet ground state, and thus may

(14) Pariser, R. *J. Chem. Phys.* **1956**, *24*, 250–268.
(15) The structures with odd *n* and *n* > 1 present an apparent violation of the rule[8] that in alternant hydrocarbons with unequal numbers of starred and unstarred atoms, the NBMO's are confined to the larger set. However, this rule was derived for structures with only two NBMO, while **3**$_3$ and **3**$_5$ have four and six NBMOs, respectively.

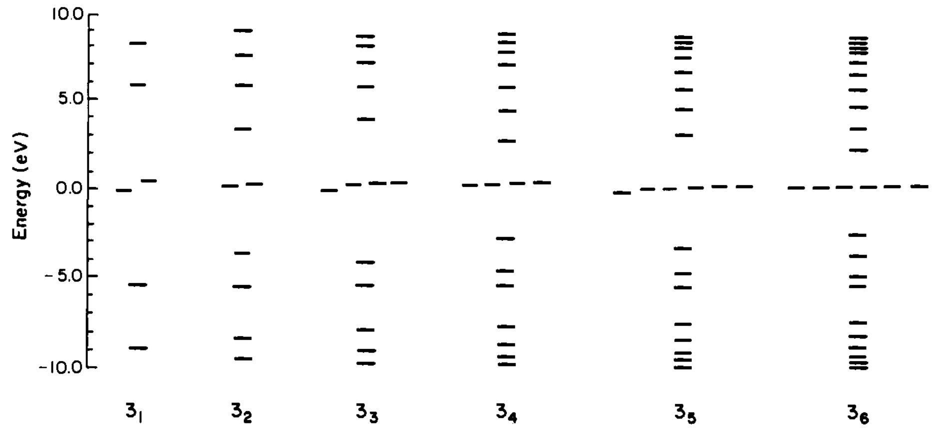

Figure 3. PPP SCF orbital energies for 3_1–3_6.

Table IV. Calculated Electronic Transitions[a] for 3_2

	NSCI	NSDCI	2-level SCI	3-level SCI	4-level SCI
		Triplet Transitions			
$B_{3u} \rightarrow B_{3u}$ (forbidden)	*b*	*b*	766	755	758
$B_{3u} \rightarrow A_g$ (allowed)	*b*	*b*	592 (0.004)	661 (0.001)	623 (0.0)
$B_{3u} \rightarrow B_{1g}$ (allowed)	842 (0.010)	840 (0.010)	635 (0.011)	637 (0.007)	584 (0.006)
$B_{3u} \rightarrow B_{2u}$ (forbidden)	819	816	624	623	572
$B_{3u} \rightarrow A_g$ (allowed)	*b*	*b*	474 (0.002)	498 (0.001)	492 (0.002)
		Singlet Transitions			
$A_g \rightarrow A_g$ (forbidden)	*b*	*b*	409	492	493
$A_g \rightarrow B_{1g}$ (forbidden)	597	596	453	414	444
$A_g \rightarrow B_{2u}$ (allowed)	596 (0.011)	594 (0.010)	455 (0.009)	417 (0.005)	443 (0.005)
$A_g \rightarrow B_{3u}$ (allowed)	*b*	*b*	*b*	415 (0.0)	429 (0.003)
$A_g \rightarrow A_g$ (forbidden)		429	367	366	355

[a] In nm; values in parentheses are oscillator strengths. [b] No configurations of excited-state symmetry at this level of theory.

not be detectable by ESR spectroscopy. Given this result, the remarkable accuracy of the PPP–CI prediction of the electronic transition in 3_1 becomes especially important to our experimental efforts to synthesize and detect 3_2. One might expect that PPP–CI should also provide a reasonable estimate of the electronic transitions in 3_2, and we have calculated both singlet and triplet transitions at several levels of theory. The results are summarized in Table IV.

For both singlet and triplet 3_2 the first allowed electronic transitions are at substantially longer wavelengths than in analogous spin states of 3_1, as expected. Like 3_1, the first T–T transition of 3_2 is at lower energy than the first S–S transition. Not surprisingly for a more complex molecule such as this, there is some scatter among the various methods. Nevertheless, we feel that the prediction of weak (symmetry allowed, parity forbidden) transitions at ca. 580–640 nm for triplet 3_2 and 420–460 nm for singlet 3_2 will provide valuable guideposts for our experimental efforts.

The Infinite Non-Kekulé Acene: Polycyclobutadiene

Given the intense current interest in conducting polymers and related structures, one cannot avoid considering the structure 3_n with $n = \infty$. As n gets larger, the effects of the "end groups" (the CH_2's) should become negligible, and in the limit one is left with polycyclobutadiene. We have performed standard band structure calculations on polycyclobutadiene at the level of HMO theory.[16] While the infinite polymer is not the major emphasis of this work, we will briefly summarize the HMO predictions of its band structure.

The results for polycyclobutadiene are summarized in Figure 5. Along with a low-lying, completely filled band and a high-lying empty band, there are two bands of intermediate energy that cross (Figure 5a). The origin of these middle bands is easily deduced. They both arise from the NBMO's of cyclobutadiene. The band

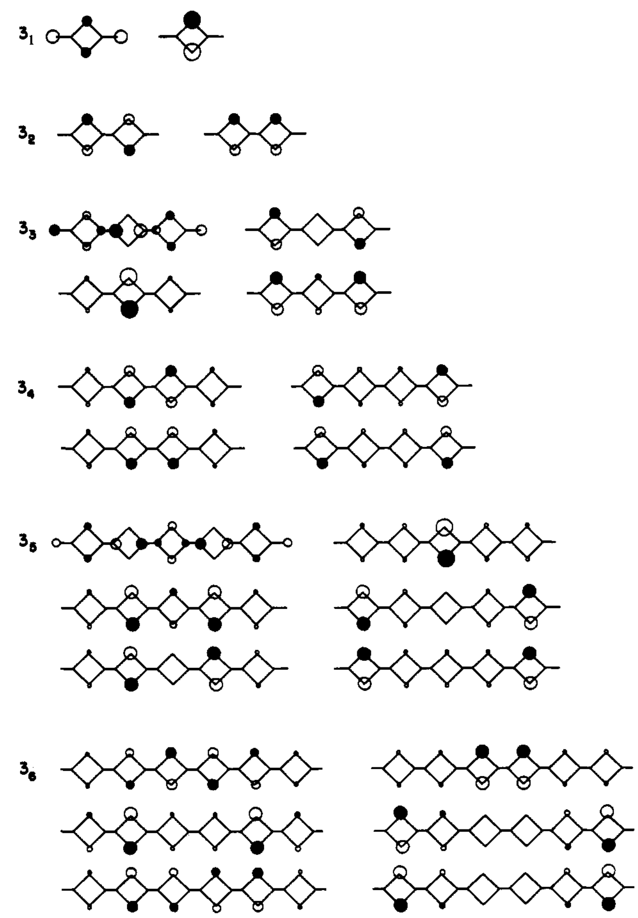

Figure 4. NBMO's for 3_1–3_6.

that shows a considerable dispersity (i.e., ranges from 1.00 to −1.00 β) results from the left NBMO of **4**, which produces significant

(16) For an excellent introduction to calculations of this sort, see: Albright, T. A.; Burdett, J. K.; Whangbo, M. H. *Orbital Interactions in Chemistry* Wiley: New York, 1985; pp 229–257.

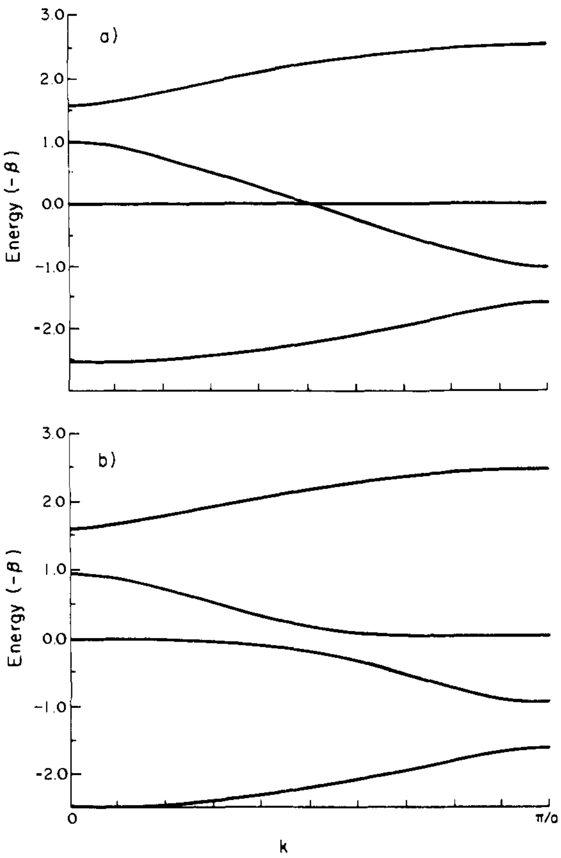

Figure 5. HMO band structure of polycyclobutadiene: (a) regular polycyclobutadiene (all bond integrals equal); (b) polycyclobutadiene with bond alternation.

intercell interactions. As Figure 5a shows, the fully "in-phase" combination of this orbital ($k = 0$) has only antibonding intercell interactions and is thus the energy maximum of the band. The other band (Figure 5a) is completely degenerate (zero dispersity) and arises from the right NBMO of **4**. There is no dispersion in this band because, at the level of HMO, there are no intercell interactions. Of course, this band is just the infinite extension of the n degenerate NBMO's of $\mathbf{3}_n$ when n is even.

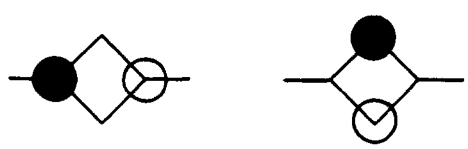

4

The band structure of Figure 5a is quite extraordinary, the most unusual property being the presence of an infinitely narrow, half-filled band at the Fermi level. This is an example of "superdegeneracy," a notion recently developed by Hughbanks.[17] One would expect that such a structure should undergo a Peierls distortion analogous to the bond alternation seen in polyacetylene. We have crudely modeled the expected distortion by considering structure **5**. In **5**, the HMO bond integrals between atoms that are shown as sharing a double bond were set to 1.1 β, while those between atoms sharing a single bond (including the intercell connections) were set to 0.9 β. This gives the band structure of Figure 5b. The lowest and highest bands are barely affected, but the NBMO's of **4** mix, and the crossing between the middle bands is "avoided." Even with this distortion, the band structure is very intriguing with a very narrow band gap,[18] a high-lying Fermi level, and relatively broad valence and conduction bands.

(17) Hughbanks, T. *J. Am. Chem. Soc.* **1985**, *107*, 6851–6859.

(18) For comparison, a similar calculation on polyacetylene (i.e., 0.9 and 1.1 β) gives a band gap of 0.4 vs. 0.008 β for **5**.

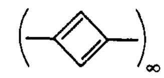

5

Discussion

Non-Kekulē molecules have been the focus of much research effort in recent years, with one of the major goals being the development of simple methods for predicting the basic properties of such structures. The non-Kekulē acenes provide a fertile testing ground for the various methods. If we consider the PPP results to be semiquantitatively reliable, then a straightforward qualitative approach emerges. HMO theory correctly predicts the number of NBMO's and their nodal properties. In order to determine the preferred spin states, one simply counts the numbers of starred and unstarred atoms. At least for the non-Kekulē acenes, this simple combination of an HMO calculation with a counting of starred and unstarred atoms provides qualitatively correct information. There are indications that this approach could break down for systems with more complex connectivity patterns.[10]

The underlying reason that the starred/unstarred approach is successful is that in most cases it correctly predicts whether the NMBO's are disjoint or not. Exceptions arise in structures involving unions of odd AH at inactive sites,[7] an arrangement that is not present in $\mathbf{3}_n$. It can easily be shown that even for non-Kekulē acenes with more than two NBMO's, the disjoint NBMO analysis holds. Referring to Figure 4, it is apparent that when n is even ($\mathbf{3}_4$ and $\mathbf{3}_6$), a completely disjoint set of NBMO's can be obtained simply by confining each NBMO to only one ring. There would be one such NBMO for each ring. Since all the NBMO's are disjoint, a singlet ground state is expected. When n is odd ($\mathbf{3}_3$ and $\mathbf{3}_5$), the situation is more complex. The n orbitals of A symmetry can be localized in the same manner as the NBMO's in the even n case. For the NBMO of S symmetry, a distinctive nodal pattern emerges. There are nodal planes perpendicular to the molecular axis and to the long axis, which contain the unstarred CH groups. If one numbers the rings from left to right, these nodes bisect the even-numbered rings. Using $\mathbf{3}_5$ as an example, there are two such nodal planes in the S NBMO. Clearly, the two A NBMO's that are localized into these even-numbered rings are disjoint with regard to the S NBMO, while the other three are not. One thus has a set of four NBMO's (one S and three A) that share common atoms, and two others that are fully disjoint. A perhaps naive extension of the Borden–Davidson analysis[7] places like spins in the four nondisjoint NBMO's, and the opposite spins in the two disjoint NMBO's. One would have, for example, four α spins and two β spins, thus producing a triplet state.

The present work has uncovered several interesting features of the non-Kekulē acenes, but perhaps the most intriguing is the parity rule. One can rationalize the parity rule using simple structural arguments. For non-Kekulē molecules, there are two structural prototypes. One is trimethylenemethane (TMM). It has three starred and one unstarred atoms and serves as the prototypical high-spin, non-Kekulē molecule. In fact, all high-spin, non-Kekulē molecules contain an embedded TMM substructure. The prototypical low-spin non-Kekulē molecule is tetramethyleneethane (TME), with three starred and three unstarred atoms. TME can be thought of as two allyl radicals joined at the node of the allyl NBMO. Both TMM and TME contain two NBMO's, which are disjoint in the case of TME but not in the case of TMM.

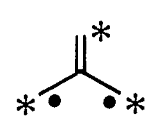

TMM

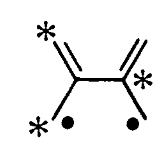

TME

The non-Kekulē acenes can be built up from these two smaller, non-Kekulē units. It is simpler to consider the even n structures

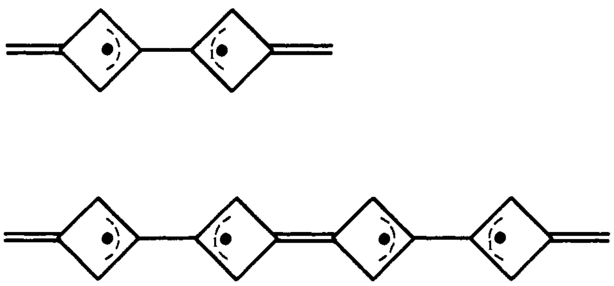

Figure 6. Even *n* non-Kekulé acenes built up from TME units.

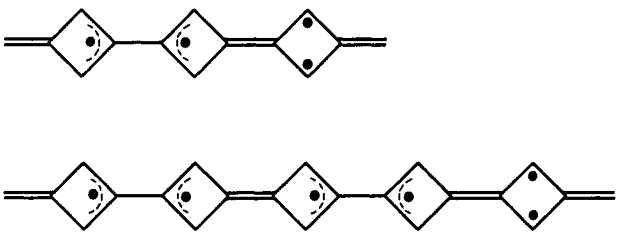

Figure 7. Odd *n* non-Kekulé acenes built up from TME units and one TMM unit.

first. The even *n*, non-Kekulé acenes can be built up entirely from TME's, as shown in Figure 6. Since TME is low spin, and since the individual TME units are insulated from one another, the whole molecule is low spin. The NBMO's of Figure 4 support this view. For even *n*, the NBMO's appear to be just linear combinations of isolated p orbitals on the CH groups. However, they are, in fact, linear combinations of allyl NBMO's, as suggested by the structures of Figure 6. In Figure 4, p orbitals in the same ring (even *n*) are *always* out of phase with one another, as expected for an allyl NBMO. If the non-Kekulé acene NBMO's were just linear combinations of isolated p orbitals, one would have expected some in-phase pairings of orbitals in the same ring.

When *n* is odd, one can build up $(n-1)/2$ TME's, leaving one remaining ring. This ring must take on the form of a TMM (Figure 7). Thus, non-Kekulé acenes with odd *n* will always have one high-spin non-Kekulé fragment, and a triplet ground state is expected. The NBMO's of Figure 4 support this analysis. There are *n* NBMO's of the allyl type. The "extra" NBMO has the form of the left member of the TMM NBMO's shown in **6**. (The right member is like an allyl NBMO.)

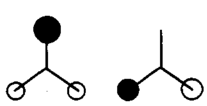

6

The simple structural analysis summarized in Figures 6 and 7 leads to correct predictions of the number of NBMO's, their nodal properties, and the ground spin states of all the non-Kekulé acenes. It also suggests another factor to be considered: nonplanarity. The barrier to rotation about the central C–C bond of TME is probably quite small, and, in fact, the ground state of TME may be an orthogonal (the two allyl units at a 90° angle) triplet.[19] This suggests another intriguing structure for the non-Kekulé acenes (**7**) with alternating eight-carbon units in

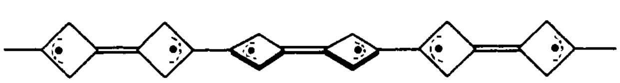

7

orthogonal planes. Conjectures about the ground state spin states

(19) Odell, B. G.; Hoffmann, R.; Imamura, A. *J. Chem. Soc. B* **1970**, 1675–1678. Dixon, D. A.; Foster, R.; Halgren, T. A.; Lipscomb, W. N. *J. Am. Chem. Soc.* **1978**, *100*, 1359–1365. Dowd, P.; Chang, W.; Paik, Y. H. *Ibid.* **1986**, *108*, 7416–7417.

Table V. PPP Parameters (eV)

core integrals	
nearest neighbor	−2.37
transannular (4-membered rings)	−0.4
electron repulsion integrals	
one-center coulomb integrals	11.35
two-center coulomb integrals	
$r \le 1.42$ Å	7.19
1.42 Å $< r \le 2.75$ Å	5.77
2.75 Å $< r \le 2.81$ Å	4.79
2.81 Å $< r$	$14.4/r$

Table VI. Results of PPP Calculations on TMM, Cyclobutadiene, and *m*-Xylylene and Comparison with Experiment and ab Initio Calculations

	PPP	ab initio	expt
	Singlet–Triplet Gaps (kcal/mol)		
TMM	13.3 (NSCI)	21.2,[a] 26.4[b]	
(T < S)	21.9 (SCI)		
	19.6 (SDCI)		
cyclobutadiene	9.2×10^{-5} (NSCI)	7.3,[c] 14.0,[d] 10[e]	
(S < T)	8.1 (SCI)		
	9.0 (SDCI)		
	Triplet–Triplet Absorption (nm)		
TMM	302 (NSCI)	266[b]	~300–350[f]
	323 (SCI)		
	339 (SDCI)		
m-xylylene	391 (NSCI)		442[g]
	451 (SDCI)		

[a] Dixon, D. A.; Dunning, T. A.; Eades, R. A.; Kleier, D. A. *J. Am. Chem. Soc.* **1981**, *103*, 2878–2880. [b] Davis, J. H.; Goddard, W. A., III. *Ibid.* **1977**, *99*, 4242–4247. [c] Kollmar, H.; Staemler, V. *Ibid.* **1977**, *99*, 3583–3587. [d] Borden, W. T.; Davidson, E. R.; Hart, P. *Ibid.* **1978**, *100*, 388–392. [e] Jafri, J. A.; Newton, M. D. *Ibid.* **1978**, *100*, 5012–5017. [f] Value for two derivatives of TMM: Turro, N. J.; Mirbach, M. J.; Harrit, N.; Berson, J. A.; Platz, M. S. *Ibid.* **1978**, *100*, 7653–7658. [g] Migirdicyan, E.; Baudet, J. *Ibid.* **1975**, *97*, 7400–7404.

and optical properties of such a structure would be highly speculative at this stage.

The many interesting predictions of the present work make the higher non-Kekulé acenes appealing experimental targets, and one can envision several viable, realistically attainable precursors. For $\mathbf{3}_2$, diazene **8** is a quite promising precursor, and our own

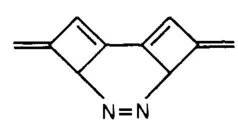

8

research group has already embarked on a rational synthesis. An alternative approach would derive from the type of precursors[4] we developed for $\mathbf{3}_1$, symbolized by **9**. One can envision several ways to oligomerize **9** into structures such as **10**. These would include, for example, oxidation (such as ozonolysis) to a mono- or diketone followed by reductive coupling, or simply olefin metathesis with removal of ethylene.

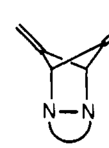

9

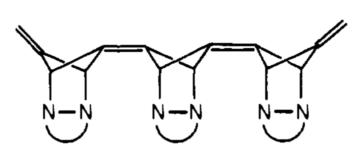

10

Conclusions

We have described structures designated by $\mathbf{3}_n$ as the non-Kekulé analogues of the classical acenes. Even the monomer ($\mathbf{3}_1$) has quite interesting electronic properties, and it is clear that the higher non-Kekulé acenes will possess fascinating optical, electronic, and magnetic properties. Perhaps most interestingly, the non-Kekulé acenes do not show a simple, progressive change in properties with increasing *n*, as do the classical acenes. Rather, a parity rule emerges, in which even n and odd n non-Kekulé acenes are expected to have qualitatively different properties. We have also shown that simple structural arguments can completely rationalize the results obtained from quantitative calculations. We are actively pursuing the experimental characterization of higher non-Kekulé acenes, in order to test the various predictions of the present work.

Acknowledgment. We thank the National Science Foundation for support of this work.

Appendix. Computational Procedures

HMO calculations were performed on an IBM PC/XT or PC/AT with the program HMO acquired from Serena Software, Bloomington, IN. The matrix diagonalization section could not solve structures with a sixfold degeneracy. This should be corrected by increasing the value of the convergence criterion, ρ.

SCF and CI calculations were performed using a PPP π-electron program[20] modified to calculate molecular orbitals for an open-shell configuration.[12] In addition to the standard parameter set,[20] we included a transannular core integral of −0.4 eV for four-membered rings.[21] The parameters are shown in Table V.

SCF calculations were performed for the non-Kekulé acenes up to $n = 6$. The molecular orbitals were optimized for a triplet state for $n = 1$ and 2, a quintet for $n = 3$ and 4, and a septet for $n = 5$ and 6. The calculations were performed using the optimized geometry of 3_1 obtained from ab initio calculations including π-space CI[13a] (square four-membered rings; ring CC bonds 1.471 Å; external CC bonds 1.374 Å).

For CI calculations four different types of CI were used. The excitations in each type of CI are (1) excitations within the NBMO's only ("NCI"), (2) excitations within the NBMO's and single excitations to and from the NBMO's ("NSCI"),[12] (3) excitations within the NBMO's and single and double excitations to and from the NBMOs ("NSDCI"), and (4) excitations within the NBMO's and all single excitations ("SCI"). Within each type of CI we also defined different "levels"; for example, a "2-level SCI" would include all single excitations involving the NBMO's and the two next-highest and two next-lowest molecular orbitals. In all the CI calculations, configurations with more than four unpaired electrons were excluded.[22]

Transition frequencies and oscillator strengths were calculated by standard methods for the transitions between the lowest triplet or singlet state and the five next-lowest states of the same multiplicity.

In order to obtain some indication of the reliability of these calculations, we performed calculations on trimethylenemethane (TMM), square cyclobutadiene, and m-xylylene. These calculations were done at regular geometries with CC bond lengths of 1.40 Å. The results of these calculations are presented in Table VI, along with values obtained by other means.

(20) Molnar, S. P. QCPE Program No. 314 Indiana University, Bloomington, IN, 1976.
(21) Wirz, J., private communication.

(22) We have also performed several calculations on 3_1 and 3_2 using all single and double excitations ("SDCI") excluding configurations with more than four unpaired electrons. The trends predicted by such calculations are in complete agreement with the "lower levels" of CI; however, the SDCI calculation may lead to an unbalanced treatment among the states. For 3_1, the only configuration with six-unpaired electrons has B_{2u} symmetry and is accessible by double excitation from the ground configuration. Exclusion of this configuration leads to a preferential destabilization of the lower lying $^3B_{2u}$ states relative to all other states. A similar imbalance exists for SDCI calculations on 3_2, and for SCI calculations for 3_3 and 3_4. For this reason, we do not consider the SDCI results to be quantitatively reliable for these structures.

MNDO Barrier Heights for Catalyzed Bicycle-Pedal, Hula-Twist, and Ordinary Cis–Trans Isomerizations of Protonated Retinal Schiff Base

Stanley Seltzer

Contribution from the Chemistry Department, Brookhaven National Laboratory, Upton, New York 11973. *Received September 15, 1986*

Abstract: Energy barriers to dark cis–trans isomerization in a protonated retinal Schiff base model in the presence and absence of electrostatic and nucleophilic catalysts have been calculated by the MNDO method. Three general processes—ordinary double bond isomerization, concerted isomerization about two double bonds by bicycle-pedal motion, and one-step double bond and adjacent single bond isomerization by hula-twist motion—are considered. Point negative charges or negatively charged nucleophiles near the protonated nitrogen substantially increase the barrier to cis–trans isomerization over what they would be in the absence of these agents. Negative charge or a nucleophile near C13 lowers the barrier to bicycle-pedal isomerization. Dark isomerization by a hula-twist motion requires greater energy and is not substantially aided by the placement of a negative charge or nucleophile near any of the skeletal atoms in the isomerizing system. The importance of this to the mechanism of dark-light adaption of bacteriorhodopsin is discussed.

Bacteriorhodopsin, the only protein within the purple membrane light-driven proton pump, binds retinal through a protonated Schiff base to its lysine-216.[1] In light-adapted bacteriorhodopsin, bound retinal molecules are in the *all-trans* form, but in the absence of light an isomerization to the 13-*cis* isomer occurs in about half of the molecules. The conversion is really a double isomerization; protonated *all-trans*,15-*anti*-retinal Schiff base isomerizes to the 13-*cis*,15-*syn* isomer.[2] It has been shown that this dark isomerization is a dynamic process with a half-life of about 40 min at ambient temperature.[3]

Another dark but faster cis–trans isomerization takes place in the main body of the bacteriorhodopsin photocycle. Following the first step wherein *all-trans*-retinal is photoisomerized to its 13-*cis* isomer, bound retinal must be rapidly reisomerized to the

(1) For a recent review see: Stoekenius, W.; Bogomolni, R. A. *Annu. Rev. Biochem.* **1982**, *52*, 587–616.

(2) Harbison, G. S.; Smith, S. O.; Pardoen, J. A.; Winkel, C.; Lugtenburg, J.; Herzfeld, J.; Matheis, R.; Griffin, R. G. *Proc. Natl. Acad. Sci. U.S.A.* **1984**, *81*, 1706–1709.
(3) Seltzer, S.; Zuckermann, R. *J. Am. Chem. Soc.* **1985**, *107*, 5523–5525.

0002-7863/87/1509-1627$01.50/0